Global Journal of Engineering and Technology Advances
eISSN: 2582-5003
Cross Ref DOI: 10.30574/gjeta
Journal homepage: https://gjeta.com/

(RESEARCH ARTICLE)

Check for updates

Experiments on Digital Filtering of Analog Signals: Pulse Amplitude Modulation and Delta Modulation

Abdul Rasak Zubair *

Department of Electrical and Electronic Engineering, University of Ibadan, Ibadan, Oyo State, Nigeria.

Global Journal of Engineering and Technology Advances, 2023, 16(01), 083–098

Publication history: Received on 05 June 2023; revised on 25 July 2023; accepted on 28 July 2023

Article DOI: https://doi.org/10.30574/gjeta.2023.16.1.0135

Abstract

To boost students' active learning and understanding of abstract scientific concepts, hands-on learning experiences such as experiments are necessary. Computer simulations also allow students to carry out experiments virtually. Analog signals are processed using digital signal processing because of the advantages of digital signal processing over analog signal processing. Numerical experiments, results, and observations on digital band pass filtering of analog signals are presented. Two types of digital modulation are employed: Pulse Amplitude Modulation (PAM) and Delta Modulation (DM). Results demonstrated higher suppression of frequencies in the stopband compared with the transition band. Frequencies in the passband suffer minimum or no attenuation. The phase difference between input and output signals, transient response, and steady state response are observed vividly. PAM is found to add less noise to the system compared with DM. These experiments are recommended as virtual laboratory exercises for undergraduate and postgraduate studies for active learning purposes.

Keywords: Active learning; Virtual laboratory; Digital modulation; Digital filter; Waveform; Transient response

1. Introduction

An experiment is a scientific procedure undertaken to make a discovery, test a hypothesis, or demonstrate a known fact [1,2]. Science experiments are used as scientific investigations to provide answers to a question through observation and experimentation [3]. To boost students' active learning and understanding of abstract scientific concepts, interactive hands-on learning experiences such as investigation and experiments are necessary [1,4,5]. Experiments can provide insight into the "cause" and the “effect” by demonstrating what outcome occurs when a particular factor is varied [6]. Virtual laboratories where students can perform experiments remotely are supporting distance learning education [7,8]. Computer simulations also allow students to carry out experiments virtually [9,10,11]. Many topics and many areas of specialization in the Electrical and Electronic Engineering discipline are adaptable for computer simulations.

The topic of interest in this paper is the digital filtering of analog signals. Most real-life signals are analog in nature. Analog signals can be processed using digital signal processing because of the advantages of digital signal processing over analog signal processing. These advantages include higher accuracy, lower cost, flexibility, ease of signal storage, and time sharing. Even though digital signal processing has the disadvantages of higher power consumption and complexity, it is still better than analog signal processing [12,13,14]. Digital signal processing operations are addition, subtraction, and shifting which are easily simulated using the Digital computer.

The complexity arises because there is a need for analog to digital conversion (ADC) and digital to analog conversion (DAC) as illustrated in Fig. 1 for digital band pass filtering of analog signals. The ADC involves digital or pulse modulation and the DAC involves digital or pulse demodulation. Modulation is the translation of an information-bearing signal or

* Corresponding author: Abdul Rasak Zubair; Email: ar.zubair@ui.edu.ng

modulating signal to a higher frequency. A parameter of the carrier signal is modified by the instantaneous amplitude of the modulating signal [15,16,17]. In digital or pulse modulation, the carrier is also known as a sampling signal and it is a train of pulses. There are many types of digital or pulse modulation techniques such as Pulse Amplitude Modulation (PAM), Pulse Code Modulation (PCM), Delta Modulation (DM), and Pulse Width Modulation (PWM); just to mention a few [14,16,17,18,19]. PAM and DM are considered for digital modulation in this work.

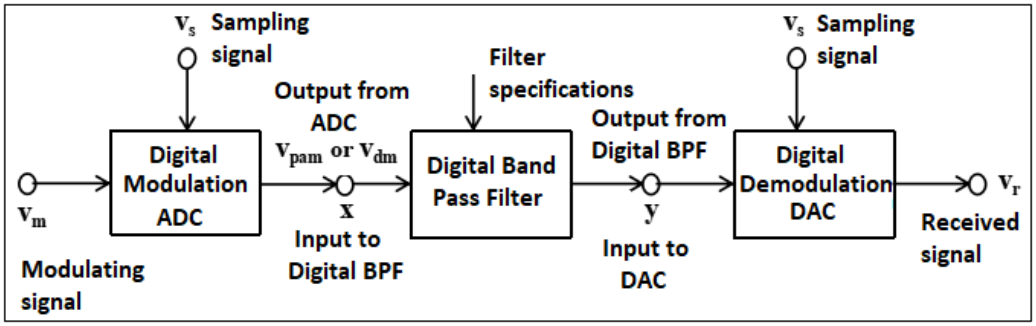

Figure 1 Digital Signal Processing of Analog Signals

A digital band pass filter passes a range of frequencies and block frequencies that are greater than or less than the range of frequencies. Digital filter design remains an active area of research [5,12,13,14,20,21]. Numerical experiments are conducted on digital band pass filtering of analog signals with two types of digital modulation (PAM and DM). The aim is to demonstrate and provide insight into the working of filtering through experimental observations. Certain factors are fixed, certain factors are varied, measurements are made, and observations/results are recorded and discussed.

2. Material and methods

2.1. Digital Band Pass Filter

An elliptic digital band pass filter (BPF) was designed using bilinear transformation based on guidelines in [5] and [20] with specifications stated in Table 1. As shown in Fig.1, x and y are the input and output respectively for the digital BPF. The filter's function is given by (1). At any given digital frequency w_d, H(z) can be evaluated as a complex quantity having magnitude ($|H(z)|$) and phase (θ_f) as shown in (2). The Gain of the filter, $Gain_f$ is given by (3). $Gain_f$ is associated with the ratio of y and x in the z domain. θ_f is the phase difference between y and x.

Table 1 Digital Band Pass Filter Specifications

Normalized Analog Low Pass Filter Specifications	
$\boldsymbol{w_{pass} = 1}$ rad/sec	$\boldsymbol{w_{stop} = 2}$ rad/sec
$\boldsymbol{A_{pass} = -3}$ dB	$\boldsymbol{A_{stop} = -50}$ dB
Sampling Signal Frequency and Period	
$\boldsymbol{f_s = 500}$ kHz	$\boldsymbol{T_s = 1/500000}$ sec
Analog Cut Off Frequencies	
$\boldsymbol{f_{c1} = 3}$ kHz	$\boldsymbol{w_{c1} = 1.8850\ x\ 10^4}$ rad/sec
$\boldsymbol{f_{c2} = 10}$ kHz	$\boldsymbol{w_{c2} = 6.2832\ x\ 10^4}$ rad/sec
Equivalent Digital Cut Off Frequencies	
$\boldsymbol{w_{dc1} = 0.0377}$ rad/sec	
$\boldsymbol{w_{dc2} = 0.1255}$ rad/sec	

$$H(z) = \frac{Y(z)}{x(z)} = \frac{\begin{matrix}0.0012z^{0}-0.0096z^{-1}+0.0329z^{-2}-0.0650z^{-3}+0.0809z^{-4}-0.0650z^{-5}\\ +0.0329z^{-6}-0.0096z^{-7}+0.0012z^{-8}\end{matrix}}{\begin{matrix}z^{0}-7.9281z^{-1}+27.5255z^{-2}-54.6617z^{-3}+67.9095z^{-4}-54.0477z^{-5}\\ +26.9106z^{-6}-7.6640z^{-7}+0.9558z^{-8}\end{matrix}} \quad \ldots\ldots\ldots\ldots\ldots \quad (1)$$

where $z = e^{jw_d}$, w_d (rad/sec) is the digital frequency which is equivalent to the analog frequency w (rad/sec) or f_m (Hz), and $w = 2\pi f_m$.

$$H(z) = |H(z)| < \theta_f \quad \ldots\ldots\ldots\ldots\ldots \quad (2)$$

$$Gain_f = 20log\left|\frac{Y(z)}{X(z)}\right| = 20log|H(z)| \quad \ldots\ldots\ldots\ldots\ldots \quad (3)$$

The frequency response of the filter is presented in Fig. 2. Bilinear transformation is associated with frequency warping which maps analog frequency w rad/sec (or f_m Hz) to digital frequency w_d rad/sec and vice versa according to (4) and (5). Fig. 2 shows both the digital frequency w_d and analog frequency f_m (horizontal axis). The marks for w_d have uniform spacing unlike those for f_m. The filter's function (1) is converted to the filter's difference equation as in (6). Given the input sequence x(n), the output sequence y(n) can be computed using (6). The Gain of the overall system of Fig. 1 is $Gain_s$. $Gain_s$ is given by (7). $Gain_s$ is associated with the ratio of the output analog signal or received signal v_r and the input analog signal or modulating signal v_m in the s domain. θ_s is the phase difference between v_r and v_m.

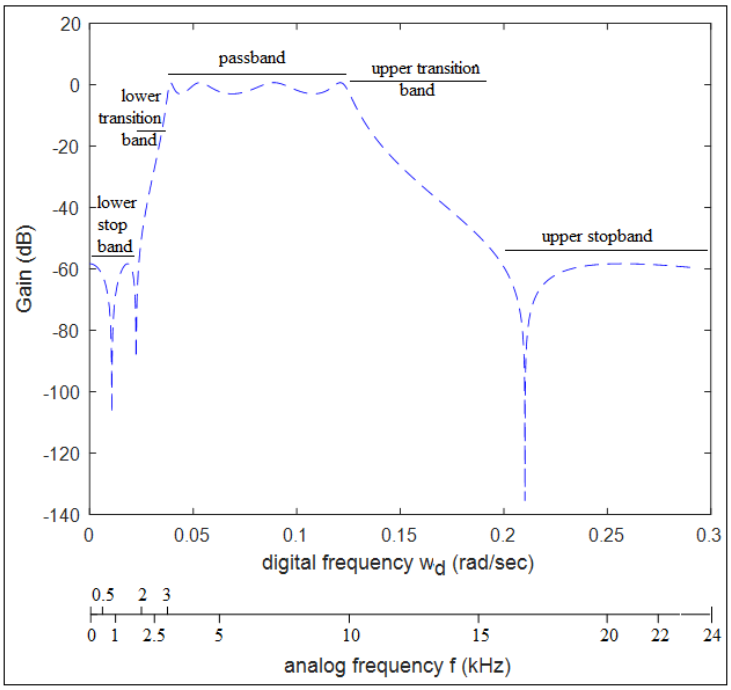

Figure 2 Frequency Response of the Digital Band Pass Filter

$$w = \frac{2}{T_s}\tan\left(\frac{w_d}{2}\right) \quad \ldots\ldots\ldots\ldots\ldots \quad (4)$$

$$w_d = 2\tan^{-1}\left(\frac{T_s w}{2}\right) \quad \ldots\ldots\ldots\ldots\ldots \quad (5)$$

$$y(n) = 7.9281y(n-1) - 27.5255y(n-2) + 54.6617y(n-3) - 67.9095y(n-4) + 54.0477y(n-5)$$

$$-26.9106y(n-6) + 7.6640y(n-7) - 0.9558y(n-8) + 0.0012x(n) - 0.0096x(n-1)$$

$$+0.0329x(n-2) - 0.0650x(n-3) + 0.0809x(n-4) - 0.0650x(n-5) + 0.0329x(n-6)$$

$$-0.0096x(n-7) + 0.0012x(n-8) \quad \ldots\ldots\ldots\ldots\ldots \quad (6)$$

$$Gain_s = 20log\left|\frac{V_r(s)}{V_m(s)}\right| \quad \ldots\ldots\ldots\ldots\ldots\ldots \quad (7)$$

2.2. Analog Test Signals

The test analog input signal is given by (8). A_m is kept constant as 2 Volts. Eight values of f_m were selected as shown in Table 2. Therefore, there are eight test signals which cut across the lower stopband, lower transition band, passband, upper transition band, and upper stopband frequency ranges which are indicated in Fig. 2.

$$v_m(t) = A_m Sin(2\pi f t) \quad \ldots\ldots\ldots\ldots\ldots\ldots \quad (8)$$

Table 2 Test Signal Frequencies

Test Freq (kHz)	band	range
0.5	lower stopband	$< f_{c1}$
1		
2.5	lower transition band	$< f_{c1}$ & close to f_{c1}
7	passband	$> f_{c1}$ & $< f_{c2}$
9		
11.5	upper transition band	$> f_{c2}$ & close to f_{c2}
16	upper stopband	$> f_{c2}$
25		

2.3. Delta Modulation based ADC and DAC

Fig. 3(a) shows the block diagram of the delta modulation subsystem (ADC). The modulating signal v_m and the feedback stepwise approximation signal v_b are illustrated in Fig. 3(d). The comparator compares v_b with v_m at every sampling instance. When v_m is greater than v_b, the encoder outputs a positive pulse of magnitude D for the delta modulated signal v_{dm}. When v_m is less than v_b, the encoder outputs a negative pulse of magnitude -D for the v_{dm} signal. D is fixed as 2 V. The delta modulated signal v_{dm} is shown in Fig. 3(c). Whenever the v_{dm} signal is positive or negative, the integrator increases or decreases v_b by a constant ss (step size) respectively.

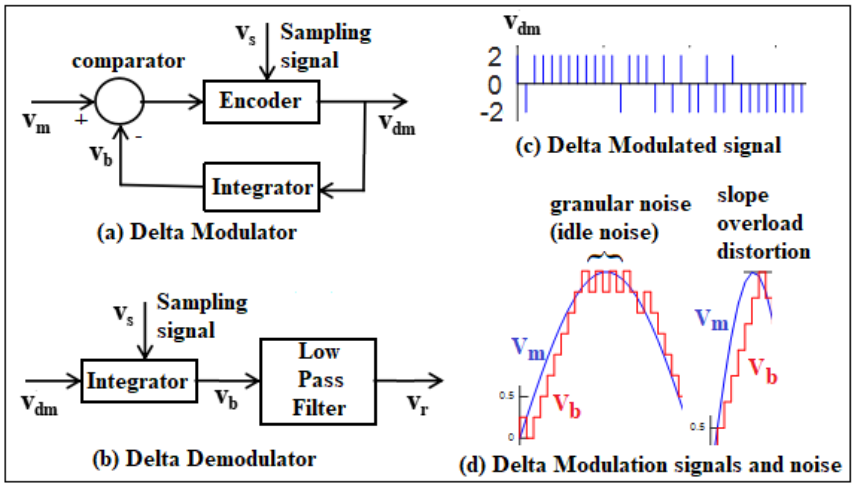

Figure 3 Delta Amplitude Modulation Subsystem and Signals

Delta modulation has three types of noise: quantization noise, granular or idle noise, and slope overload distortion [22]. Quantization noise is the difference between the values of v_m and v_b at any sampling instance. Granular or idle noise occurs when the variations in the input signal v_m are too small compared with the step size (ss) as illustrated in Fig. 3(d). Fig. 3(d) also shows the slope overload distortion which occurs when the variations in the input signal v_m are too

high compared with the step size (ss) and v_b could not follow v_m correctly. The step size is regulated by (9) to avoid slop overload distortion.

$$ss = 2\pi f A_m / f_s \quad \ldots\ldots\ldots\ldots\ldots\ldots \quad (9)$$

The output of the integrator in the delta demodulation subsystem (DAC) of Fig. 3(b) is the stepwise approximation signal v_b which is given by (10). v_b in the delta demodulation subsystem of Fig. 3(b) will be equal to the v_b in the delta modulation subsystem of Fig. 3(a) if and only if the exact v_{dm} from the modulation subsystem is delivered as input to the demodulation subsystem. The low pass filter in Fig. 3(b) converts the step-wise approximation signal v_b to the received signal v_r. Sampling frequency far higher than the Nyquist rate is required to minimize noise; f_s is chosen as 500 kHz as indicated in Table 1.

$$v_b(n) = v_b(n-1) + ss\frac{v_{dm(n)}}{D} \quad \ldots\ldots\ldots\ldots\ldots\ldots \quad (10)$$

2.4. Pulse Amplitude Modulation based ADC and DAC

Fig. 4 shows the pulse amplitude modulator and the pulse amplitude modulated signal. The instantaneous amplitude of the modulating signal v_m appears as the pulse amplitude modulated signal v_{pam} output at every sampling instance. The pulse amplitude demodulator is a low pass filter that detects the envelope of the tips of the PAM samples as the received signal v_r.

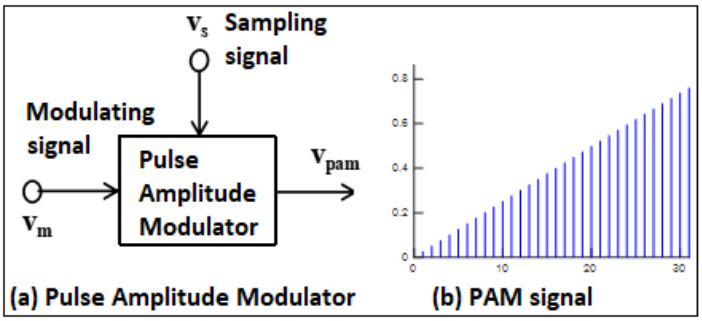

Figure 4 Amplitude Modulation Subsystem and Signals

2.5. Calculation of the Filter's $Gain_f$ and Phase Difference θ_f

For any given modulating signal frequency f_m, the equivalent digital frequency w_d is calculated with the help of (5). The filter's $Gain_f$ and θ_f are calculated by substituting w_d in (1), (2), and (3).

2.6. Experimental Estimation of the Filter's $Gain_f$

The filter's $Gain_f$ can be estimated experimentally by finding the mean of the squares of the elements in the sequences x(n) and y(n). These mean values are substituted in (11) proposed in this work. The 0^{th} to 10000^{th} samples are used for the sequence x(n); a total of 10,001 samples. The 5000^{th} to 10000^{th} samples are used for the sequence y(n); a total of 5,001 samples. Only later samples of y(n) are used as it is certain that the output y(n) would have reached the steady state by $n = 5000$. The initial samples of y(n) may contain transient responses. Many samples are used so that the averages can be as accurate as possible.

$$Gain_f = 10log_{10}\left[\frac{10001\sum_{n=5000}^{n=10000}[y(n)]^2}{5001\sum_{n=0}^{n=10000}[x(n)]^2}\right] \quad \ldots\ldots\ldots\ldots\ldots\ldots \quad (11)$$

2.7. Experimental Estimation of the System's $Gain_s$ and Phase Difference θ_s

There are no formulas for calculating the system's $Gain_s$ and θ_s. The presence of the ADC and the DAC will not allow the system's $Gain_s$ to be exactly equal to the filter's $Gain_f$; the two may be close to each other. Similarly, the system's phase difference θ_s will not be exactly equal to the filter's phase difference θ_f; the two may be close to each other. The $Gain_s$ can be estimated like the $Gain_f$ in (11) and as described by (12).

$$Gain_s = 10log_{10}\left[\frac{10001\sum_{n=5000}^{n=10000}[v_r(nT_s)]^2}{5001\sum_{n=0}^{n=10000}[v_m(nT_s)]^2}\right] \quad \ldots\ldots\ldots\ldots\ldots\ldots \quad (12)$$

The system's phase difference θ_s can be estimated from the data or graph of v_m and v_r as illustrated in Fig. 5 and as described by (13) proposed in this work. N1 is the number of sample points within a period of v_m. N2 is the number of sample points between two points where v_m and v_r cross from a negative value to zero. N1 represents the phase difference θ_s and N2 represents a complete cycle or a period of v_m which is 2π radians. θ_s is negative as v_r lags behind v_m as seen in Fig. 5. N1 and N2 are measured when the system has reached steady state. It is better to measure N1 and N2 at several locations and the averages of these quantities are used in (13).

$$\theta_S = 2\pi \frac{N1}{N2} \qquad \ldots\ldots\ldots\ldots\ldots\ldots \qquad (13)$$

2.8. Software Implementation

The software realization of the Analog to Digital Converters (ADC: DM and PAM), the Digital Band Pass Filter (BPF), and the Digital to Analog Converters (DAC) were developed in terms of computer programs in MATLAB. Additional programs to visualize the waveforms of the various signals, calculate $Gain_f$ and θ_f, and estimate $Gain_f$, $Gain_s$, and θ_s were also developed in MATLAB.

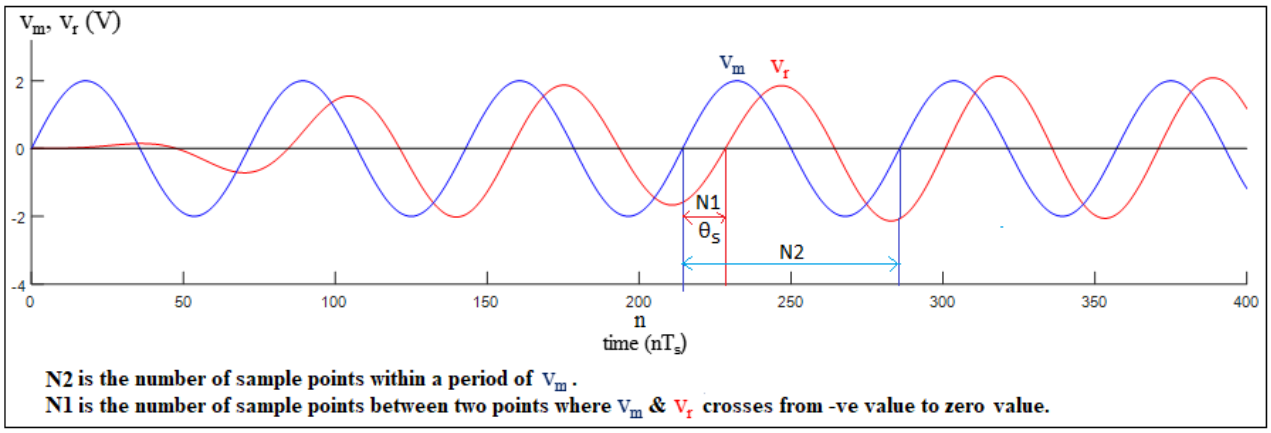

Figure 5 Experimental graphical estimation of the system's phase difference θ_s

3. Results and discussion

3.1. Delta Modulation Subsystem

To study the working of the delta modulation subsystem alone, the digital band pass filter was excluded from the system of Fig. 1. The output of the delta modulator (ADC) was sent directly to the delta demodulator (DAC). The modulating signal v_m with f_m equal to 7 kHz, the delta modulated signal v_{dm}, the stepwise approximation signal v_b, and the demodulated signal or received signal v_r were observed and recorded as presented in Fig. 6. The received signal v_r closely follows the modulating signal v_m.

3.2. Pulse Amplitude Modulation Subsystem

To study the working of the amplitude modulation subsystem alone. The digital band pass filter was excluded from the system of Fig. 1. The output of the pulse amplitude modulator (ADC) was sent directly to the pulse amplitude demodulator (DAC). The modulating signal v_m with f_m equal to 7 kHz, the pulse amplitude modulated signal v_{pam}, and the demodulated signal or received signal v_r are shown in Fig. 7. The received signal v_r is the same as the modulating signal v_m.

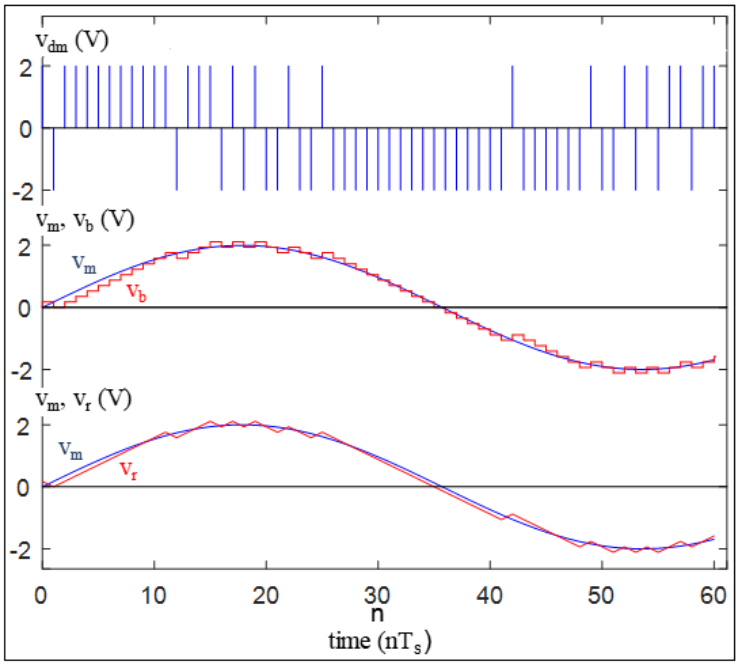

Figure 6 Delta Modulation Signals for 7 kHz test frequency

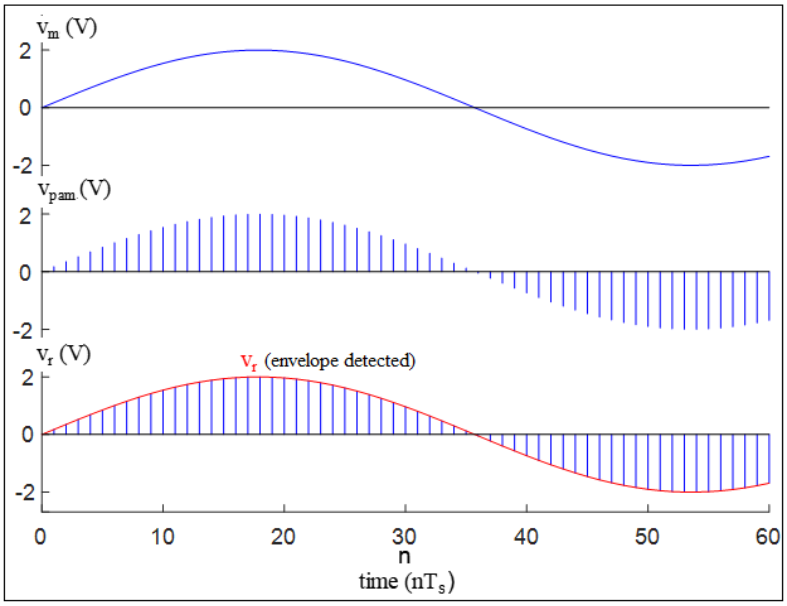

Figure 7 Pulse Amplitude Modulation Signals for 7 kHz test frequency

3.3. Digital Band Pass Filtering System with Delta Modulation Based ADC and DAC.

The digital filtering system with delta modulation (DM) based ADC and DAC was tested with the eight analog test signals. Transient response is observed in the output sequence y(n) and received signal v_r. The initial samples $(0 \leq n \leq N_{transient})$ are characterized by extremely smaller or higher signal transient values which are normal for electrical circuits and networks. The response of a system is considered to be its steady state response $(n > N_{transient})$ when the transient response would have decayed to zero. $N_{transient}$ is not the same for the test signals.

The results for the 1 kHz test frequency are presented in Fig. 8. The output sequence y(n) and the received signal v_r are negligible in the steady state. Hence the signal is suppressed because its frequency falls in the stopband range.

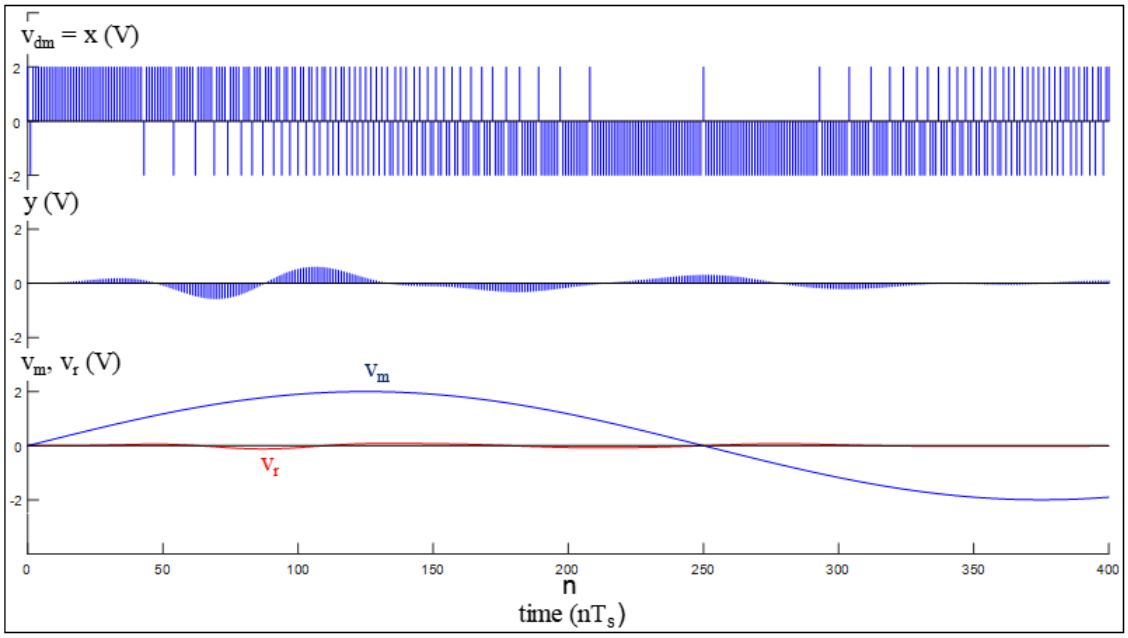

Figure 8 DM stopband results: waveforms of v_m, v_r, v_{dm}, x, and y for 1 kHz test frequency

Fig. 9 shows the received signal v_r for the test frequencies 0.5 kHz, 1 kHz, 16 kHz, and 25 kHz which are in the stopband. In all cases, the peak-to-peak value of v_r ranges from 0.02 V to 0.26 V in the steady state $(n > N_{transient} \approx 400)$. These peak-to-peak values are far less than the peak-to-peak value of the input signal v_m which is 4 V. The system, therefore, suppresses frequencies in the stopband.

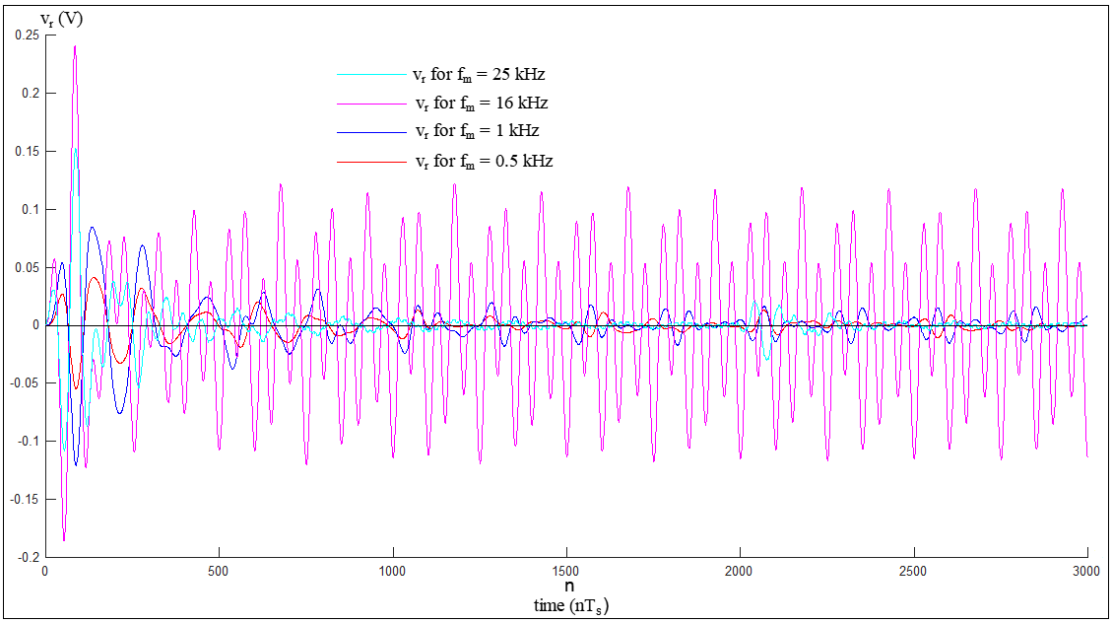

Figure 9 DM Stopband results: waveforms of v_r for 0.5 kHz, 1 kHz, 16 kHz, and 25 kHz test frequencies

The results for the 2.5 kHz test frequency are presented in Fig. 10. The output sequence y(n) and the received signal v_r are limited in the steady state. Hence the signal is somehow suppressed because its frequency falls in the transition band range.

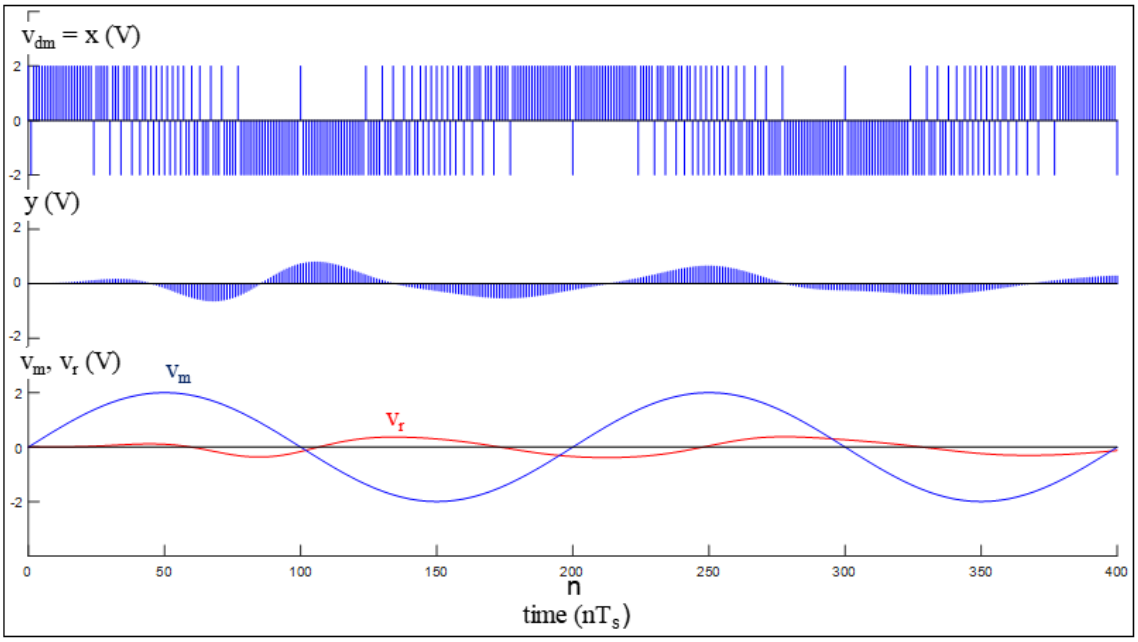

Figure 10 DM transition band results: waveforms of v_m, v_r, v_{dm}, x, and y for 2.5 kHz test frequency

Fig. 11 shows the received signal v_r for the test frequencies 2.5 kHz and 11.5 kHz which are in the transition band. In both cases, the peak-to-peak value of v_r ranges from 0.2 V to 0.4 V in the steady state ($n > N_{transient} \approx 600$). These peak-to-peak values are less than the peak-to-peak value of the input signal v_m which is 4 V. The degree of suppression of frequencies in the transition band is significant but it is less than the degree of suppression of frequencies in the stopband.

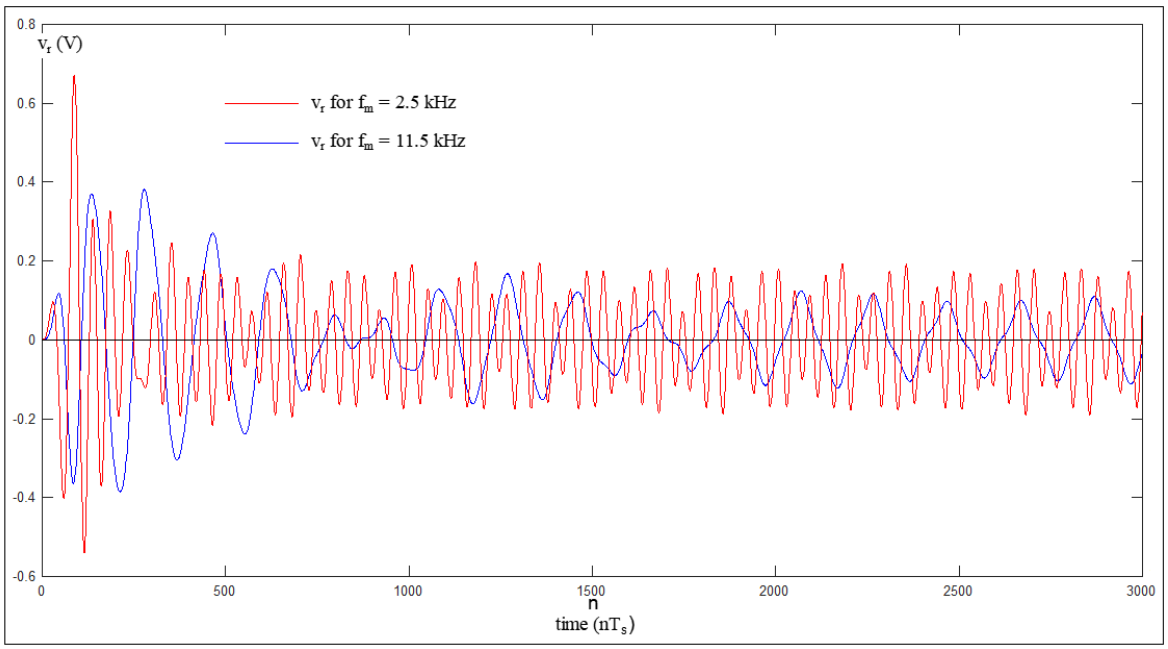

Figure 11 DM transition band results: waveforms of v_r for 2.5 kHz and 11.5 kHz test frequencies

The results for 7 kHz and 9 kHz test frequencies are displayed in Figs. 12 and 13. In both cases, the output sequence y(n) and the received signal v_r are very significant and are close to x(n) and v_m respectively in magnitude. Hence these test signals are allowed to pass with minimum or no attenuation because their frequencies fall in the passband range. For the 7 kHz, N1, N2, and θ_s are estimated as 14.33, 71.40, and -1.2610 rad/sec respectively. v_r lags behind v_m. For the 9 kHz, N1, N2, and θ_s are estimated as 27.89, 55.57, and 3.1535 rad/sec respectively. v_r leads v_m.

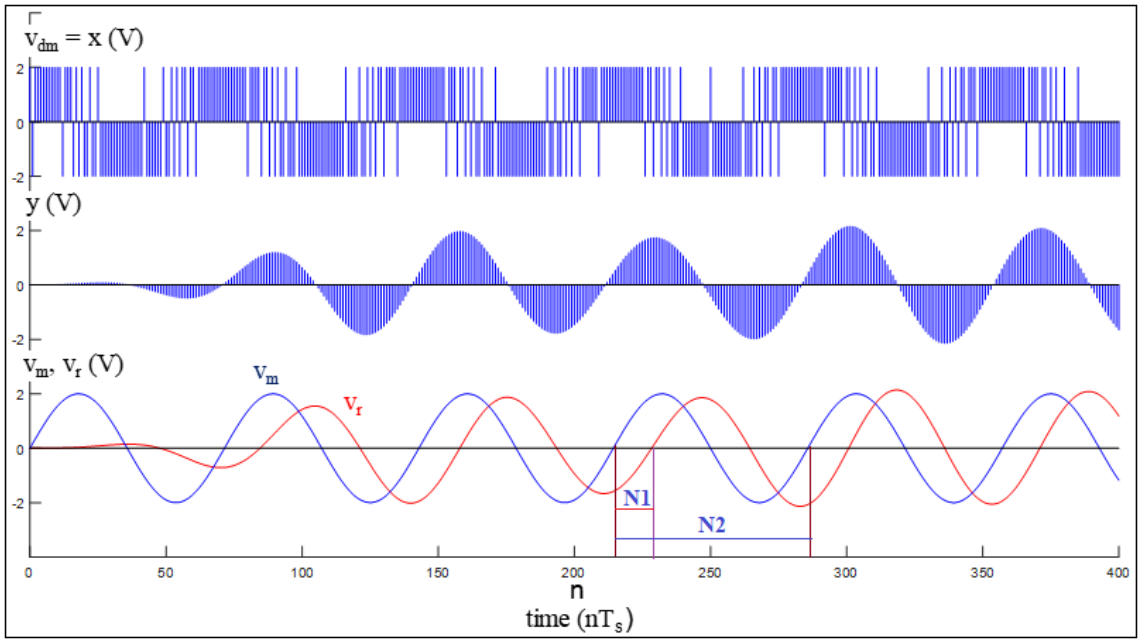

Figure 12 DM passband results: waveforms of v_m, v_r, v_{dm}, x, and y for 7 kHz test frequency

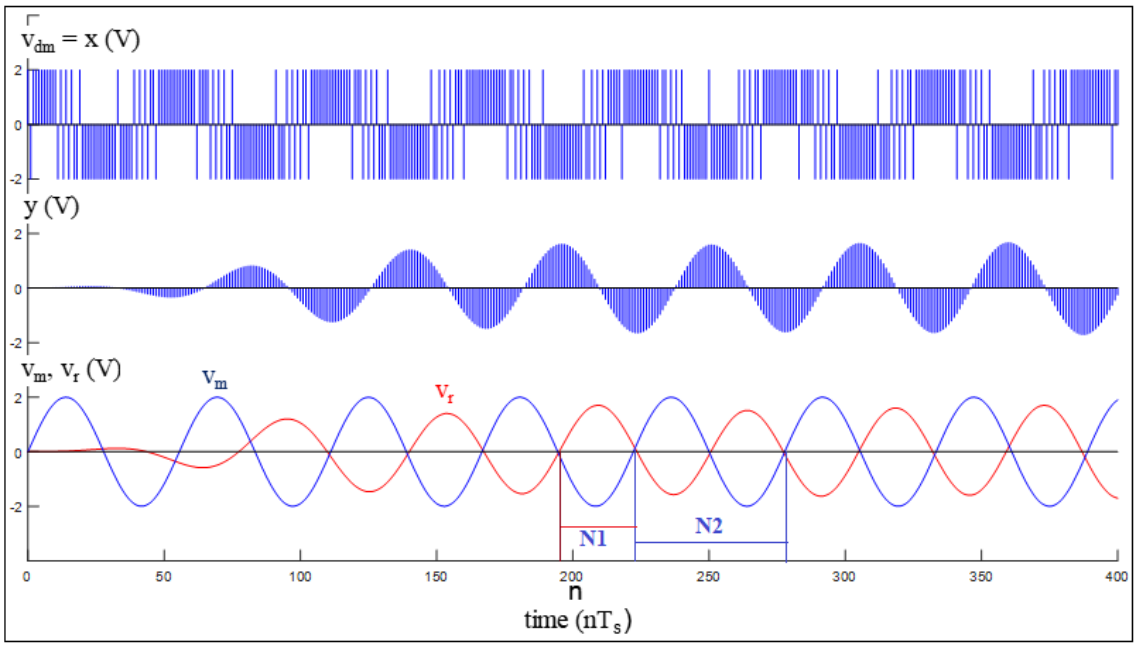

Figure 13 DM passband results: waveforms of v_m, v_r, v_{dm}, x and y for 9 kHz test frequency

3.4. Digital Band Pass Filtering System with Pulse Amplitude Modulation Based ADC and DAC.

The digital filtering system with pulse amplitude modulation (PAM) based ADC and DAC was tested with the eight analog test signals. Transient response is also observed in the output sequence y(n) and received signal v_r. The results for 1 kHz test frequency are presented in Fig. 14. The output sequence y(n) and the received signal v_r are negligible in the steady state. Hence the signal is suppressed because its frequency falls in the stopband range.

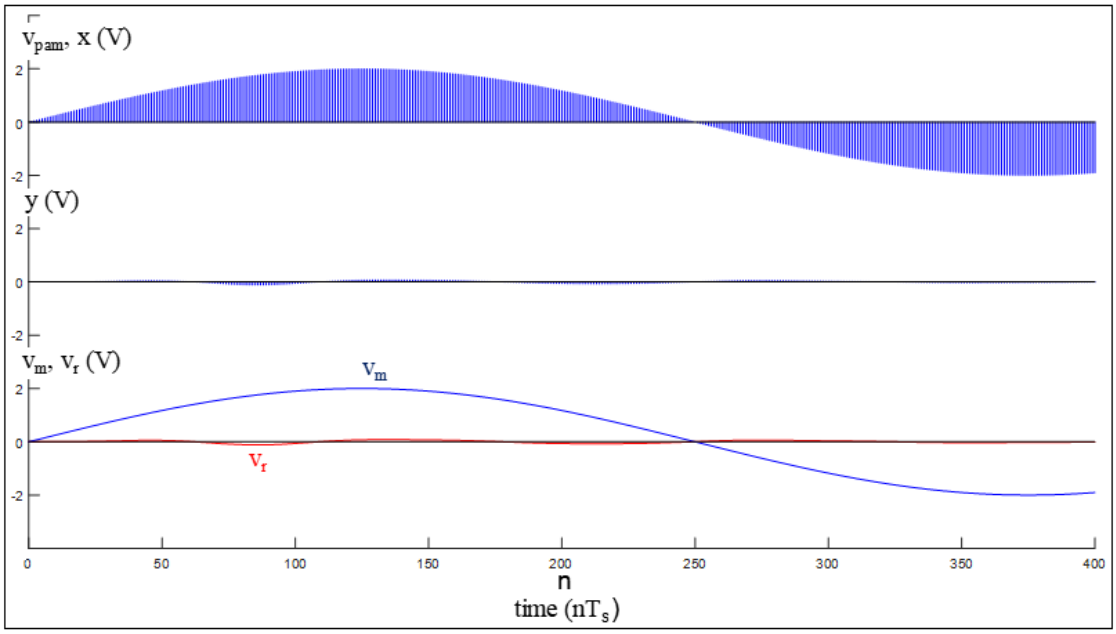

Figure 14 PAM stopband results: waveforms of v_m, v_r, v_{pam}, x, and y for 1 kHz test frequency

Fig. 15 shows the received signal v_r for the test frequencies 0.5 kHz, 1 kHz, 16 kHz, and 25 kHz which are in the stopband. In all cases, the peak-to-peak value of v_r is less than 0.05 V in the steady state ($n > N_{transient} \approx 400$). These peak-to-peak values are far less than the peak-to-peak value of the input signal v_m which is 4 V. The system, therefore, suppresses frequencies in the stopband.

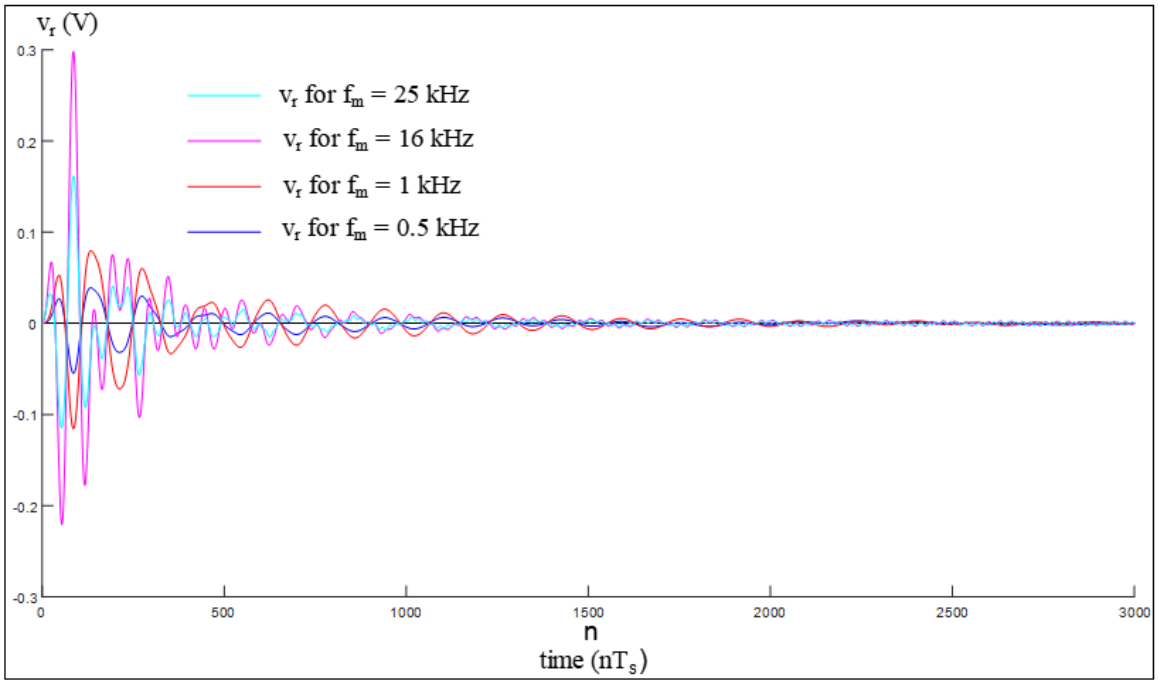

Figure 15 PAM stopband results: waveforms of v_r for 0.5 kHz, 1 kHz, 16 kHz, and 25 kHz test frequencies

The results for the 2.5 kHz test frequency are presented in Fig. 16. The output sequence y(n) and the received signal v_r are limited in the steady state. Hence the signal is somehow suppressed because its frequency falls in the transition band range.

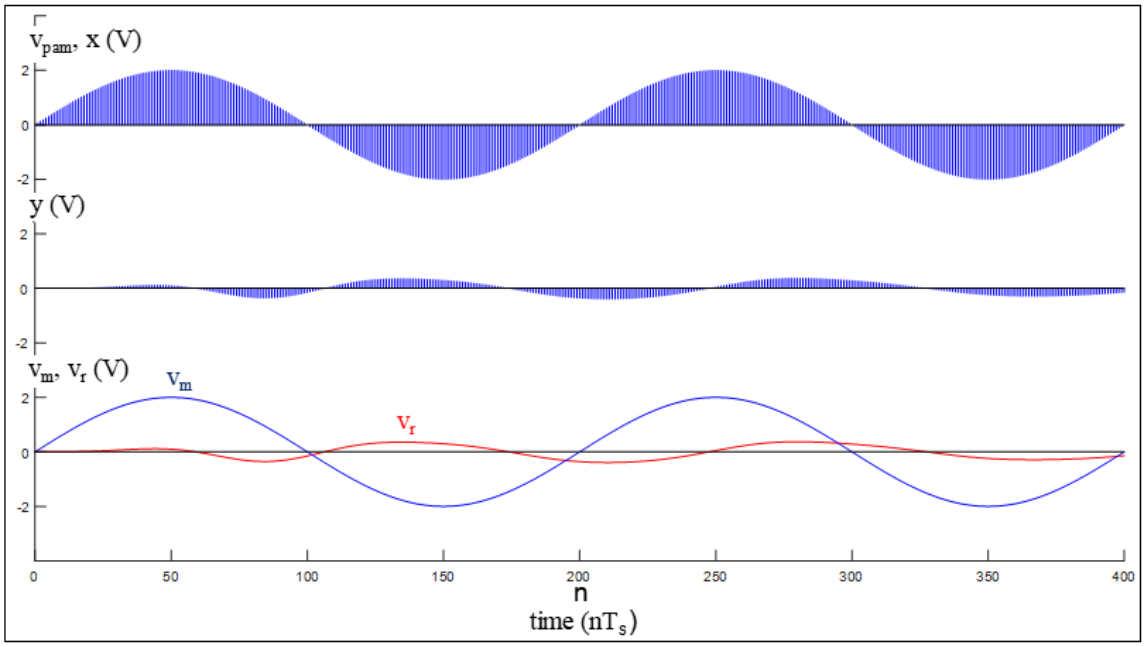

Figure 16 PAM transition band results: waveforms of v_m, v_r, v_{pam}, x, and y for 2.5 kHz test frequency

Fig. 17 shows the received signal v_r for the test frequencies 2.5 kHz and 11.5 kHz which are in the transition band. In both cases, the peak-to-peak value of v_r ranges from 0.1 V to 0.3 V in the steady state ($n > N_{transient} \approx 700$). These peak-to-peak values are less than the peak-to-peak value of the input signal v_m which is 4 V. The degree of suppression of frequencies in the transition band is significant but it is less than the degree of suppression of frequencies in the stopband.

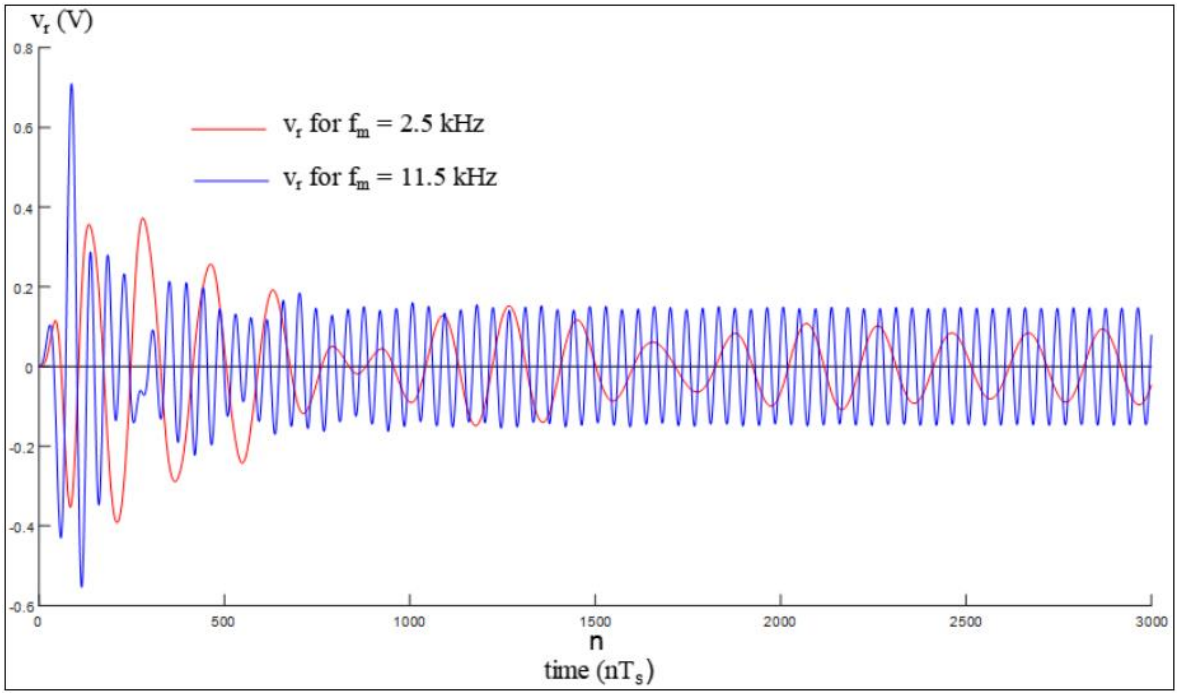

Figure 17 PAM transition band results: waveforms of v_r for 2.5 kHz and 11.5 kHz test frequencies

The results for 7 kHz and 9 kHz test frequencies are displayed in Figs. 18 and 19. In both cases, the output sequence y(n) and the received signal v_r are very significant and are close to x(n) and v_m respectively in magnitude. Hence these test signals are allowed to pass with minimum or no attenuation because their frequencies fall in the passband range.

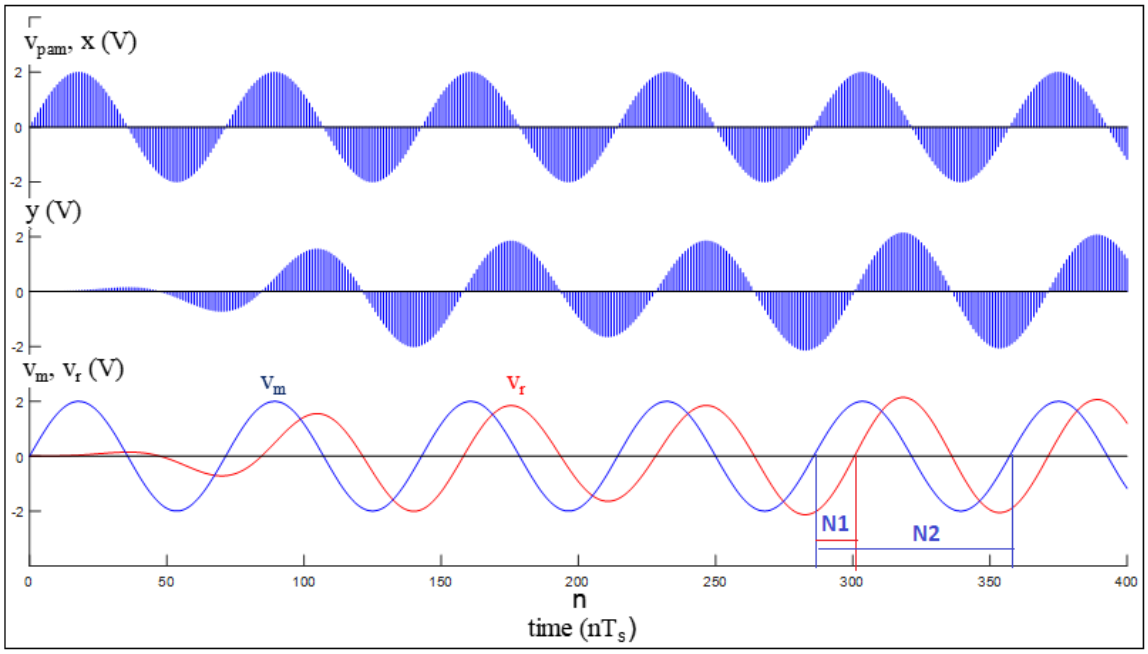

Figure 18 PAM passband results: waveforms of v_m, v_r, v_{pam}, x, and y for 7 kHz test frequency

For the 7 kHz, N1, N2, and θ_s are estimated as 14.75, 71.45, and -1.2970 rad/sec respectively. v_r lags behind v_m. For the 9 kHz, N1, N2, and θ_s are estimated as 27.90, 55.57, and 3.1545 rad/sec respectively. v_r leads v_m.

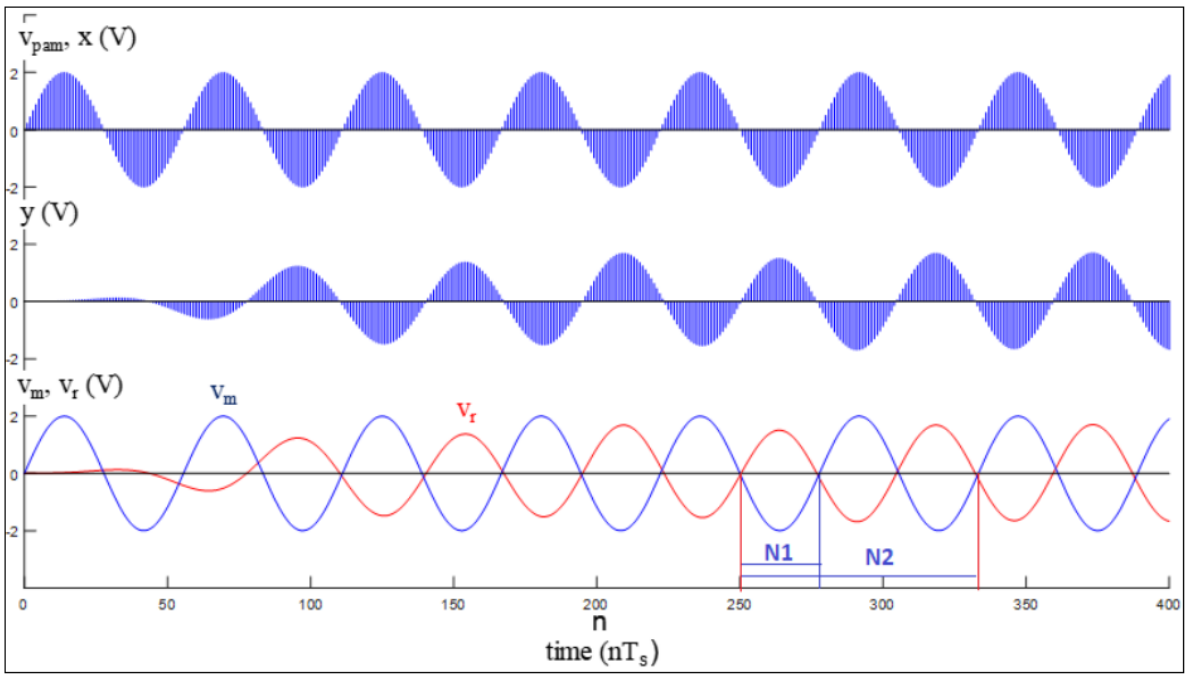

Figure 19 PAM passband results: waveforms of v_m, v_r, v_{pam}, x, and y for 9 kHz test frequency

3.5. Comparison of DM and PAM

The delta modulation and the pulse amplitude modulation performed equally well in the digital filtering system for analog signals. The results are comparable and the waveforms of the received signal are similar. Table 3 shows the calculated values of the filter's $Gain_f$ and phase difference θ_f which are the same for both the DM and the PAM systems. The estimated filter's $Gain_f$, over all system's $Gain_s$, and phase difference θ_s for the DM and PAM are also presented in Table 3.

Table 3 Calculated and Estimated Gain and Phase Difference

					DM Based ADC & DAC			PAM Based ADC & DAC		
		Calculation			Estimation			Estimation		
Analog Freq		Digital Freq	Digital BPF		Digital BPF	Complete System		Digital BPF	Complete System	
f_m	w	w_d	$Gain_f$	θ_f	$Gain_f$	$Gain_s$	θ_s	$Gain_f$	$Gain_s$	θ_s
kHz	rad/sec	rad/sec	dB	rad	dB	dB	rad	dB	dB	rad
0.5	3141.6	0.00628	-62.32	-0.0608	-33.63	-51.61	-	-62.41	-62.41	-
1.0	6283.2	0.01257	-68.21	-3.2685	-32.09	-45.86	-	-68.29	-68.29	-
2.5	15708.0	0.03141	-26.78	-0.4988	-28.86	-26.76	-	-26.86	-26.86	-
7.0	43982.4	0.08791	0.62	-1.2547	-2.43	0.58	-1.2610	0.54	0.54	-1.2970
9.0	56548.8	0.11298	-2.41	3.3398	-5.52	-2.50	3.1535	-2.47	-2.47	3.1545
11.5	72257.0	0.14430	-22.41	0.5683	-25.58	-22.33	-	-22.68	-22.68	-
16.0	100531.2	0.20039	-59.83	0.2815	-34.74	-26.93	-	-60.71	-60.71	-
25.0	157080.0	0.31161	-61.13	-2.9853	-57.96	-47.18	-	-61.43	-61.43	-

Colour Key

stopband | passband | transition band

The estimated $Gain_f$ for PAM is closer to the calculated $Gain_f$ for all test frequencies compared with DM. The estimated $Gain_s$ is equal to the estimated $Gain_f$ for PAM but the estimated $Gain_s$ is less than the estimated $Gain_f$ for DM. DM introduces more error or noise in the system compared with PAM.

It was observed that the received signal v_r does not have the same frequency as the input signal v_m for the stopband and transition band frequencies. Therefore, phase difference θ_s could only be estimated for passband frequencies.

4. Conclusion

A software system for the digital filtering of analog signals has been developed and subjected to rigorous experimental tests. Two different digital modulation techniques are employed: delta modulation and pulse amplitude modulation. Experimental calculation, estimation, and observations provided lots of insights into the theory and application of delta modulation, pulse amplitude modulation, and digital filtering. The experiments confirmed the concepts of transient response and steady state response. Pulse amplitude modulation is found to add less noise to the system compared with delta modulation. These experiments are recommended as virtual laboratory exercises for undergraduate and postgraduate studies for active learning purposes.

Compliance with ethical standards

Acknowledgments

The author would wish to acknowledge the Electrical and Electronic Engineering Department, University of Ibadan, Ibadan, Nigeria.

Disclosure of conflict of interest

There are no conflicts of interest in this manuscript.

References

[1] Oxford, Oxford Languages, retrieved from https://languages.oup.com/google-dictionary-en/ on 20 February 2023.

[2] Merriam-Webster, Dictionary, retrieved from https://www.merriam-webster.com/dictionary/experiment on 20 February 2023.

[3] Sanskruti World School, Why you should teach students with science experiments, retrieved from https://www.sanskrutividyasankul.com/why-you-should-teach-students-with-science-experiments/ on 13 March 2023.

[4] National Education Association (NEA), Getting Hands-On to Learn About Science and Nature, retrieved from https://www.nea.org/advocating-for-change/new-from-nea/getting-hands-learn-about-science-and-nature on 13 March 2023.

[5] Zubair AR, Olawale AJ. Active learning strategy: Computer aided numerical class project on pole-zero plot and transfer function of five low pass filter approximation functions. Global Journal of Engineering and Technology Advances. 2022; 12 (1): 038-063.

[6] Freeman S, Eddy SL, McDonough M, Wenderoth MP. Active learning increases student performance in Science, Engineering and Mathematics.Psychological and Cognitive Sciences. 2014; 111 (23): 8410-8415.

[7] Tsichouridis Ch, Vavougios D, Batsila M, Ioannidis GS. The Optimum Equilibrium when Using Experiments in Teaching – Where Virtual and Real Labs Stand in Science and Engineering Teaching Practice. International Journal of Emerging Technologies in Learning (iJET). 2019; 14 (23): 67-84.

[8] Lockett H. Using remote laboratory experiments to develop learning outcomes in engineering practice. In: Horizons in STEM Higher Education Conference: Making Connections, Innovating and Sharing Pedagogy, 1-2 Jul 2020, University of Nottingham – virtual.

[9] Başer M, Durmuş S. The Effectiveness of Computer Supported Versus Real Laboratory Inquiry Learning Environments on the Understanding of Direct Current Electricity among Pre-Service Elementary School Teachers. Eurasia Journal of Mathematics, Science & Technology Education. 2010; 6 (1): 47-61.

[10] Finkelstein ND, Adams WK, Keller CJ, Kohl PB, Perkins KK, Podolefsky NS, Reid S, LeMaster R. When learning about the real world is better done virtually: A study of substituting computer simulations for laboratory equipment. Physical Review Special Topics - Physics Education Research. 2005; 1 (1): 010103(1)-010103(8).

[11] van Joolingen WR, de Jong T, Dimitrakopoulou A. Issues in computer supported inquiry learning in science. Journal of Computer Assisted Learning. 2007; 23 (2): 111– 119.

[12] Proakis JG, Manolakis DG. Digital Signal Processing Principles, algorithms, and Applications. Third Edition. New Jersey, USA: Prentice-Hall, Inc ; 2012.

[13] Oppenheim AV, Schafer RW, Buck JR, Discrete-Time Signal Processing. Englewood CliFs, USA: Prentice-Hall, Inc; 1999.

[14] Smith SW. The Scientist and Engineer's Guide to Digital Signal Processing. San Diego: California Technical Publishing; 1999.

[15] Zubair AR, Folorunso SS. Education during COVID-19 lockdown and Social Distancing: Programmable Teaching Aid for Amplitude Modulation Theory as a Case Study. International Journal of Computer Applications. 2020; 175 (33): 11-29.

[16] Sinha U. Principles of communication. New Delhi: Satya Prakashan; 1988.

[17] Kenney G, Davis B. Electronic Communication Systems. New Delhi: Tata McGraw-Hill Publishing Company; 1992.

[18] Holmes DG, Lipo TA. Pulse Width Modulation for Power Converters: Principles and Practice. USA: IEEE Press Series on Power Engineering; 2003.

[19] Zubair AR. Numerical Integration Based Analysis of Pulse Width Modulated Voltage Source Inverter. In A. Gyasi-Agyei and T. Ogunfunmi (Eds.). Adaptive Science and Technology: Proceedings of the 2nd IEEE International Conference on Adaptive Science and Technology (ICAST), Accra, Ghana, 14-16 December 2009.

[20] Zubair AR, Olawale AJ. From First Principles to Patterns to Arithmetic/Logical Operations: Computer Aided Digital Filter Design with Bilinear Transformation. In Z. Hu et al. (Eds,). Chapter 31, Advances in Computer

Science for Engineering and Education VI, LNDECT 181. Proceedings of the 6th International Conference on Computer Science, Engineering and Education Applications, Warsaw, Poland, 17 - 19 March 2023. Switzerland: Springer Nature. DOI:10.1007/978-3-031-36118-0_31.

[21] Thede L. Practical Analog and Digital Filter Design. Ohio: Artech House Inc; 2004.

[22] Engineering Made Easy, Delta Modulation Noise, retrieved from https://www.engineeringmadeeasypro.com/2018/06/Slope-Overload-Distortion-and-Granular-Noise-Quantization-Noise-in-Delta-Modulation.html on 13 March 2023.